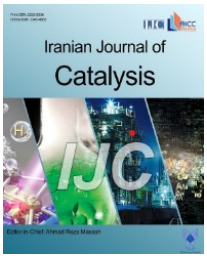

Iran. J. Catal. 2026; 16(2): 284-298

Iranian Journal of Catalysis (IJC)

https://doi.org/10.57647/ijc.2026.1602.18

Research Article

Hercynite@SiO_2-APTS-Proline as a Novel Magnetic Nanocatalyst for the Regioselective Synthesis of New Spiro[indoline-3,5'-pyrido-pyrimidine/dipyrimidine] Derivatives

Haniyeh Bozorgi Siyahestalkhi, Hassan Kefayati*, Mohammad Nikpassand

Department of Chemistry, Ra.C., Islamic Azad University, Rasht, Iran

*Corresponding authors: ha.kefayati@iau.ac.ir

Article History:

Received:
21 November 2025

Revised:
05 January 2026

Accepted:
10 February 2026

Published Online:
11 May 2026

Published in Issue:
30 June 2026

Abstract

Hercynite ($FeAl_2O_4$) magnetic nano particle (MNP) was prepared by a chemical coprecipitation process and the surface of its functionalized with amino propyl tetramethyl Silan (APTS) groups. Reaction of synthesized Hercynite@SiO_2-APTS with proline was obtained Hercynite@APTS-Proline as a new nanoparticle. The structure and composition of the synthesized Hercynite@APTS-Proline characterized by FT-IR, XRD, EDX, SEM, TEM, TGA and VSM techniques. The catalytic activity of prepared Hercynite@APTS-Proline was used for the synthesis of spiro [indoline-3,5'-pyrido[2,3-*d*] pyrimidine] and spiro[indoline-3,5'-pyrido[2,3-d:6,5-*d'*]dipyrimidine derivatives and the results show that its catalytic activity is better than other catalysts used. In addition, the synthesized catalyst can be easily separated and reused up to 5 times without any noticeable change in the reaction yield.

Keywords: Hercynite; Nanocatalyst; Pyrido[2,3-*d*] pyrimidine; [pyrido[2,3-*d*:6,5-*d'*]dipyrimidine; Proline; Spiro compound

Cite this article: H. B. Siyahestalkhi, H. Kefayati, M. Nikpassand, Iran. J. Catal. **16** (2026) 284-298. https://doi.org/10.57647/ijc.2026.1602.18

1. Introduction

The pyrimidine structure is a key skeleton found in many known drugs. Among them pyrimidine-fused heterocycles such as pyrido-pyrimidines are important derivatives of organic compounds that have various biological and medicinal properties such as anti-tumor, anti-viral, anti-oxidant, antifungal [1-10]. The indole structure is also a well-known heterocycle that is found in many natural and medicinal compounds [11]. Furthermore, the spiro-oxindole constitutes the essential framework of various pharmacological agents and natural alkaloids [12]. In addition, it has been observed that incorporating the indole 3-carbon atom during the creation of spiro oxindole derivatives can greatly enhance their biological activity [13]. Also, spirocyclic frameworks is found in many natural and medicinal compounds [14]. In synthesis of this skeleton, chemists often face serious challenges, as its synthesis requires special design and strategy because there is a possibility of rearrangement into other organic compounds [15]. For this reason, the synthesis of these compounds has always been of interest to chemists, and numerous reports have been presented in this field [16-18].

L-proline has been used as a useful catalyst in many organic reactions due to its several structural features. *L*-proline, due to its two functional groups, amine and acid, behaves as both a Bronsted acid and a base in many reactions, or exhibits both behaviors during the same mechanism.

Also, the presence of amino and carboxylic acid groups in the vicinity makes it an excellent chelating agent and therefore forms metal chelates in metal-catalyzed reactions. On the other hand, because it is chiral, it can be used to synthesize chiral compounds with high stereoselectivity [19].

Multicomponent reactions are recognized as very powerful tools in synthetic organic and medicinal chemistry for the synthesis of the complex products in a single step from simple starting materials. The combination of magnetic nanocatalysts and multicomponent reactions will become an emerging strategic research area and is an ideal blend for the development of sustainable methods in green synthetic chemistry [20-25].

Based on this, in this research and in continuing our efforts to synthesize of spiro oxindole [26-28] and pyrido-pyrimidine compounds [29], and synthesis of new nano-catalyst for the synthesis of organic compound [30-34], as well as the widespread use of proline as a catalyst in organic reactions, We designed nano catalyst Hercynite@SiO_2-APTS-Proline as a novel and efficient catalyst by immobilization of proline on the surface of hercynite as a magnetic nanoparticle support.

Then, these nanoparticles were efficiently applied as efficient and reusable catalyst for the synthesis of novel spiro[indoline-3,5'-pyrido[2,3-*d*] pyrimidine] (SIPP) and spiro[indoline-3,5'-pyrido[2,3-*d*:6,5-*d'*]dipyrimidine (SIPDP) derivatives.

2. Materials and methods

2.1. Characterization

The chemicals and solvents used were purchased from the Merck of Germany and domestic companies. The progress of the reaction was monitored by TLC using silica gel 60, F265 mercury-coated aluminum plates. The melting temperature of the synthesized compounds was measured by the electrothermal apparatus 9200.

Infrared spectra were recorded on a KBr tablet with a spectrophotometer between the 8900 Shimadzu model and the nuclear magnetic resonance spectra (^{13}C NMR, ^{1}H NMR) with a Broker device, 250 and 400 MHz in a DMSO-d_6 solvent.

Chemical shifts (δ) were measured in ppm relative to the TMS internal reference. Elemental analysis was carried out on a Thermo Finnigan Flash EA 1112 series instrument.

2.2. General procedure for synthesis of N-alkyl isatin

Isatin (1 mmol, 0.14 g) was dissolved in DMF (3 mL) and potassium carbonate (1.3 mmol, 0.179 g) added to it and mixed together. Then, alkyl halide (1.2 mmol) was added to the reaction mixture and heated at 100 °C. After 75 minutes, the reaction mixture was passed through filter paper while hot and then the filtered solution was cooled, the precipitate formed was separated and washed several times with water and at the end recrystallized by ethanol.

2.3. Preparation of Hercynite MNPs

Hercynite ($FeAl_2O_4$) MNPs were prepared by a chemical coprecipitation process according to previous reported method [35]. A mixture of $FeCl_2$. $4H_2O$ (4 mmol, 0.5 g) and $Al(NO_3)_3$. $9H_2O$ (2 mmol. 0.5 g) was dissolved in 1000 mL of distilled water and stirred at 80 ºC under nitrogen gas. Then 10 mL of 0.2 M soda solution was added to the reaction mixture until the pH of the reaction mixture reached to 12. After stirring the mixture for 30 minutes, hercynite nanoparticles were collected with an external magnet. It was washed several times with deionized water and ethanol and then dried in an oven at 75 ºC for 4 hours.

2.4. Preparation of proline supported on the surface of hercynite ([Hercynite@SiO_2-APTS-proline])

The SiO_2 shell was encapsulated on the surface of prepared hercynite to obtain Hercynite@SiO_2 MNPs in accordance with previously reported methods for $FeAl_2O_4$ surface modification [36]. Hercynite@SiO_2 MNPs were functionalized with aminopropyl groups by mixing the prepared Hercynite@SiO_2 MNPs (1g), 3-aminopropyltrimethoxysilane (APTS; 5 mmol) and dry toluene (40 mL) in a round-bottom flask. The mixture was stirred for 24h at room temperature. Then, the Hercynite@APTS-Proline was synthesized by refluxing a mixture of proline, Hercynite@SiO_2-APTS and acetonitrile as solvent for 8h in the presence of triethylamine. Finally, Hercynite@SiO_2-APTS-Proline MNPs were separated by a magnet (1.4 T) (Scheme 1).

2.5. General method for the synthesis of SIPP (4) and SIPDP (5)

A mixture of 6-aminouracile (1 mmol. 0.127g), methyl cyanoacetate or barbituric acid (1 mmol), isatin derivatives (1 mmol) and Hercynite@SiO_2-APTS-Proline (0.07 g) as catalyst in 5 mL ethanol was refluxed/sonicated. After the reaction is complete (monitored by thin-layer chromatography), the 7'-amino-2,2',4'-trioxo-2',3',4',8'-tetrahydro-1'*H*-spiro[indoline-3,5'-pyrido[2,3-*d*]pyrimidine]-6'-carbonitrile derivatives

10.57647/ijc.2026.1602.18

(4a–h) or 10',10a'-dihydro-1'*H*-spiro[indoline-3,5'-pyrido[2,3-d:6,5-*d'*]dipyrimidine] 2,2',4',6',8'(3'H,4a'*H*,7'*H*,9'*H*)-pentaone (9a-e) were precipitated. To isolate the Hercynite@SiO_2-APTS-Proline MNPs from the products, 10 mL of hot ethanol was added into the mixture, which was subsequently heated until the precipitate fully dissolved.

Following this, the magnetic nanocatalyst was separated using a magnet (1.4 T), and the mixture underwent filtration. The crude products were then allowed to cool to room temperature, separated through filtration, and crystallized from ethanol to yield the pure compounds.

2.6. Spectroscopic data

2.6.1. *Compound 4a*

FT-IR (KBr): 3440, 3402, 3068, 2954, 1708, 1652, 1629, 1463 cm^{-1}. ^1H NMR (400 MHz, DMSO-d_6): δ: 11.26 (s, 2H, NH_2), 7.81 (s, 1H, NH), 7.69 (s, 1H, NH), 7.42-7.31 (m, 4H, H-Ar), 6.61 (s, 1H, NH), 5.58 (s, 1H, NH), 3.82 (s, 3H, O-CH_3) ppm. ^{13}C NMR (100 MHz, DMSO-d_6): δ: 164.5, 161.4, 159.9 153.9, 151.1, 144.7, 141.0, 138.8, 134.1, 128.0, 127.3, 124.7, 81.7, 79.1, 49.9, 46.2 ppm. Anal. Calcd. for $C_{16}H_{13}N_5O_5$: C, 54.09; H, 3.69; N, 19.71; found: C, 54.11; H, 3.72; N, 19.69.

2.6.2. *Compound 4b*

FT-IR (KBr): 3400, 3242, 3199, 3170, 3064, 2950, 2869, 1724, 1701, 1658, 1610, 1521, 1463 cm^{-1}. ^1H NMR (250 MHz, DMSO-d_6): δ: 11.58 (brs, 2H, NH), 7.36-7.02 (m, 5H, NH, H-Ar), 6.08 (s, 1H, NH), 5.09 (s, 1H, NH), 3.21 (s, 3H, O-CH_3), 2,85 (s, 3H, N-CH_3) ppm. ^{13}C NMR (62.89 MHz, DMSO-d_6): δ: 174.5, 163.1, 158.9, 150.6, 148.7, 147.7, 144.1, 130.5, 129.4, 126.9, 123.3, 113.8, 109.4, 90.0, 49.7, 43.8, 31.6 ppm. Anal. Calcd. for $C_{17}H_{15}N_5O_5$: C, 55.28; H, 4.09; N, 18.96; found: C, 55.25; H, 4.11; N, 18.99.

2.6.3. *Compound 4c*

FT-IR (KBr): 3444, 3261, 3134 (N-H amine), 3095 (C-H Aromatic), 2894 (C-H Aliphatic), 1731 (C=O ester), 1674, 1605 (C=O amide), 1600, 1517, 1465 (C=C) cm^{-1}. ^1H NMR (250 MHz, DMSO-d_6): δ: 11.67 (brs, 2H, NH_2), 7.62-6.80 (m, 9H, H-Aromatic), 6.40 (s, 1H, NH), 5.18 (s, 1H, NH), 4.90 (m, 2H, N-CH_2), 4.84 (s, 1H, NH), 3.06 (s, 3H, O-CH_3) ppm. ^{13}C NMR (62.89 MHz, DMSO-d_6): δ: 174.8, 163.1, 159.7, 159.0, 151.1, 150.7, 147.8, 144.8, 143.3, 137.6, 136.3, 130.4, 128.8, 127.2, 123.4, 121.8, 113.6, 110.1, 107.9, 91.0, 49.7, 44.1, 43.9 ppm. Anal. Calcd. for $C_{23}H_{19}N_5O_5$: C, 62.02; H, 4.30; N, 15.72; found: C, 62.05; H, 4.28; N, 15.75.

2.6.4. *Compound 4d*

IR (KBr): 3467, 3456, 3184, 3178, 3026, 2964, 1715, 1687, 1635, 1514, 1469, 746 cm^{-1}. ^1H NMR (250 MHz, DMSO-d_6): δ: 11.73 (brs, 2H, NH_2), 8.03-6.87 (m, 7H, H-Ar), 6.25 (s, 1H, NH), 5.22 (s, 1H, NH), 5.20- 5.02 (m, 2H, CH_2), 4.82 (s, 1H, NH), 3.07 (s, 3H, O-CH_3) ppm. ^{13}C NMR (62.89 MHz, DMSO-d_6): δ: 175.0, 162.9, 159.1, 150.6, 147.8, 142.9, 133.3, 132.5, 130.7, 129.8, 129.4, 127.8, 126.9, 123.7, 113.7, 109.8, 89.8, 49.8, 43.9, 41.73 ppm. Anal. Calcd. for $C_{23}H_{17}Cl_2N_5O_5$: C, 53.71; H, 3.33; N, 13.62; found: C, 53.73; H, 3.35; N, 13.65.

2.6.5. *Compound 4e*

FT-IR (KBr): 3329, 3112, 3080, 2920, 1743, 1615, 1522, 1485, 771 cm^{-1}. ^1H NMR (250 MHz, DMSO-d_6): δ: 10.52 (s, 2H, NH_2), 10.33 (s, 2H, NH), 7.21-7.02 (m, 4H, Aromatic), 3.39 (s, 3H, O-CH_3), 3.23 (s, 3H, N-CH_3), 3.18 (s, 3H, N-CH_3) ppm. ^{13}C NMR (62.89 MHz, DMSO-d_6): δ: 170.8, 164.1, 151.3, 150.3, 144.6, 140.1, 137.2, 131.4, 129.1, 128.1, 127.7, 122.1, 121.4, 119.1, 56.0, 45.2, 30.3, 28.4 ppm. Anal. Calcd. for $C_{18}H_{17}N_5O_5$: C, 56.39; H, 4.47; N, 18.27; found: C, 56.36; H, 4.50; N, 18.25.

2.6.6. *Compound 4f*

FT-IR (KBr): 3429, 3060, 2941, 1727, 1689, 1627, 1533, 1469, 744 cm^{-1}. ^1H NMR (250 MHz, DMSO-d_6): δ: 11.13 (s, 1H, NH), 10.28–10.09 (2H, NH), 7.77-7.53 (m, 4H, Aromatic), 3.53 (s, 6H, N-CH_3), 3.33 (s, 3H, O-CH_3), 2.99 (s, 3H, N-CH_3) ppm. ^{13}C NMR (62.89 MHz, DMSO-d_6): δ: 171.6, 165.8, 162.7, 161.5, 155.8, 154.6, 151.4, 150.3, 149.6, 139.1, 133.6, 130.5, 128.8, 111.4, 58.5, 58.0, 36.2, 32.5, 31.7 ppm. Anal. Calcd. for $C_{19}H_{19}N_5O_5$: C, 57.43; H, 4.82; N, 17.62; found: C, 57.45; H, 4.83; N, 17.65.

2.6.7. *Compound 4g*

FT-IR (KBr): 3421, 3050, 2931, 1729, 1670, 1635, 1560, 1502, 756 cm^{-1}. ^1H NMR (400 MHz, DMSO-d_6): δ: 9.06 (s, 1H, NH), 7.97-6.68 (m, 11H, H-Ar, NH_2), 4.53 (dd, 2H, J = 16.0 Hz, CH_2), 3.73 (s, 3H, O-CH_3), 3.38 (s, 6H, N-CH_3), 3.24 (s, 3H, N-CH_3) ppm. ^{13}C NMR (62.89 MHz, DMSO-d_6): δ: 176.0, 162.8, 161.4, 158.6, 151.1, 143.9, 141.8, 134.3, 133.5, 133.3, 133.0, 130.6, 129.5, 129.4, 129.1, 128.2, 124.9, 123.1, 115.4, 114.8, 61.4, 56.1, 55.6, 28.9, 27.6 ppm. Anal. Calcd. for $C_{25}H_{23}N_5O_5$: C, 63.42; H, 4.90 N, 14.79; found: C, 64.45; H, 4.89; N, 14.76.

2.6.8. *Compound 4h*

FT-IR (KBr): 3342, 3238, 3020, 2923, 1730, 1671, 1642, 1562, 1442, 797 cm^{-1}. ^1H NMR (250 MHz, DMSO-d_6): δ: 10.41 (s, 1H, NH), 7.40-7.29 (m, 7H, Aromatic), 4.67

10.57647/ijc.2026.1602.18

(m, 2H, CH_2), 3.76 (s, 3H, O-CH_3), 3.71 (s, 3H, N-CH_3), 3.59 (s, 3H, N-CH_3) ppm. ^{13}C NMR (62.89 MHz, DMSO-d_6 176.4, 160.9, 151.3, 147.1, 142.2, 139.5, 138.8, 136.8, 134.3, 134.2, 128.6, 128.5, 128.0, 127.7, 127.4, 126.4, 124.8, 124.6, 122.0, 114.0, 56.1, 56.0, 42.6, 29.3, 28.0 ppm. Anal. Calcd. for $C_{25}H_{21}Cl_2N_5O_5$: C, 55.36; H, 3.90; N, 12.91; found: C, 55.39; H, 3.92; N, 12.93.

2.6.9. *Compound 9a*

FT-IR (KBr): 3440, 3234, 3116, 3060, 1726, 1691, 1649, 1612, 1539, 1510, 1431 cm^{-1}. ^{1}H NMR (250 MHz, DMSO-d_6): δ:11.56 (s, 1H, NH), 10.60 (s, 1H, NH), 10.44 (s, 1H, NH), 9.08 (s, 1H, NH), 7.13-6.86 (m, 5H, NH, H-Ar) ppm. ^{13}C NMR (62.89 MHz, DMSO-d_6): δ: 181.7, 162.4, 157.3, 152.4, 151.5, 150.3, 146.5, 135.7, 128.6, 126.9, 123.6, 121.3, 116.6, 97.6, 82.5, 50.5 ppm. Anal. Calcd. for $C_{16}H_{10}N_6O_5$: C, 52.47; H, 2.75; N, 22.94; found: C, 52.50; H, 2.78; N, 22.91.

2.6.10. *Compound 9b*

FT-IR (KBr): 3440, 3234, 3316, 3060, 2954, 1726, 1691,1649, 1539, 1510 cm^{-1}. ^{1}H NMR (250 MHz, DMSO-d_6): δ:12.03 (brs, 2H, NH), 10.81 (s, 1H, NH), 10.21 (s, 1H, NH), 9.07 (s, 1H, NH), 7.12-6.82 (m, 4H, H-Ar), 3.07 (s, 3H, N-CH_3) ppm. ^{13}C NMR (62.89 MHz, DMSO-d_6): δ: 178.0, 161.4, 159.5, 150.4, 149.4, 145.3, 144.4, 144.2, 134.7, 128.2, 123.3, 121.7, 107.3, 89.1, 56.4, 30.4 ppm. Anal. Calcd. for $C_{17}H_{12}N_6O_5$: C, 53.69; H, 3.18; N, 22.10; found: C, 53.71; H, 3.20; N, 22.08.

2.6.11. *Compound 9c*

FT-IR (KBr): 3458, 3433, 3240, 3197, 3161, 3101, 3026 (C-H Aromatic), 2953 (C-H Aliphatic), 1687 (C=O), 1726, 1701, 1664, 1612, 1521, 1465, 757, 746 cm^{-1}. ^{1}H NMR (250 MHz, DMSO-d_6): δ: 10.30 (s, 1H, NH), 9.80 (s, 1H, NH), 8.10 (s, 1H, NH), 7.93-6.37 (m, 7H, H-Ar), 5.71 (brs, 2H, NH), 4.78 (dd, 2H, J = 17.4 Hz, CH_2) ppm. ^{13}C NMR (62.89 MHz, DMSO-d_6): δ: 162.1, 159.7, 151.3, 143.9, 134.1, 132.9, 132.7, 130.7,128.9, 127.6, 123.5, 122.2, 107.3,42.3, 34.8 ppm. Anal. Calcd. for $C_{23}H_{14}Cl_2N_6O_5$: C, 52.59; H, 2.69; N, 16.00; found: C, 52.58; H, 2.71; N, 16.03.

2.6.12. *Compound 9d*

FT-IR (KBr): 3440, 3234, 3060, 2945, 1691, 1649, 1612, 1539, 1431, 754 cm^{-1}. ^{1}H NMR (250 MHz, DMSO-d_6): δ: 11.80 (s, 1H, NH), 9.25 (s, 2H, NH), 8.63-7.41 (m, 5H, NH, H-Ar), 3.34 (s, 3H, N-CH_3), 2.99 (s, 3H, N-CH_3) ppm. ^{13}C NMR (62.89 MHz, DMSO-d_6): δ:167.7, 164.0, 157.9, 153.9, 151.7, 149.9, 136.1, 134.8, 130.6, 129.1, 125.6, 123.2, 118.7, 108.4, 104.0, 53.9, 30.8, 27.4 ppm. Anal. Calcd. for $C_{18}H_{14}N_6O_5$: C, 54.82; H, 3.58; N, 21.31; found: C, 54.80; H, 3.60; N, 21.28.

2.6.13. *Compound 9e*

FT-IR (KBr): 3433, 3055, 2970, 1658, 1604, 1527, 1461, 705 cm^{-1}. ^{1}H NMR (250 MHz, DMSO-d_6): δ: 11.29 (s, 1H, NH), 9.30 (s, 2H, NH), 7.02-6.67 (m, 7H, H-Ar), 4.52 (d, 1H, J = 16.0 Hz), 4.62 (d, 1H, J = 16.0 Hz), 3.16 (s, 3H, N-CH_3), 3.30 (s, 3H, N-CH_3) ppm. ^{13}C NMR (62.89 MHz, DMSO-d_6): δ:167.8, 166.0, 164.6, 162.9, 150.6, 147.8, 144.7, 142.9, 139.0, 133.3, 132.6, 130.7, 129.8, 129.3, 127.8, 126.9, 125.1, 123.7, 117.4, 113.7, 49.8, 43.9, 31.7, 28.2 ppm. Anal. Calcd. for $C_{25}H_{18}Cl_2N_6O_5$: C, 54.26; H, 3.28; N, 15.19; found: C, 54.29; H, 3.31; N, 14.21.

3. Result and discussion

3.1. Preparation and characterization of catalysts

Hercynite with the formula $FeAl_2O_4$ and the composition of the percentage of elements 31% aluminum, 32 % iron and 37% oxygen is a black oxide mixture with a spinel structure that one out of the eight tetrahedral sites occupied with Fe^{2+} cations and one half of the octahedral sites are occupied by Al^{3+} cations [37]. Hercynite was found in chromite but due to the difficulty of extracting these pure types, in industry it is obtained through synthesis. Among the properties of hercynite, high temperature stability and chemical resistance against alkalis and sulfates can be mentioned. In this research, modified hercynite nanoparticles [Hercynite@SiO_2-APTS-Proline] were successfully prepared according to the method presented in the experimental section, as shown in Scheme 1.

Scheme 1. Synthesis of Hercynite@SiO_2-APTS-Proline

10.57647/ijc.2026.1602.18

Fig. 1 shows the FT-IR spectra of Hercynite, Hercynite@SiO_2, Hercynite@SiO_2-APTS, and Hercynite@SiO_2-APTS-Proline MNPs. In Fig. 1a, correspond to Hercynite ($FeAl_2O_4$) MNPs, absorption tape at 580–600 cm^{-1} is related to Fe–O and Al-O stretching vibrations. Moreover, bands at about 3420–3450 cm^{-1} are related to stretching vibrations of the hydroxyl and interlayer water molecules [35,38]. In Hercynite@SiO_2 spectrum (Fig. 1b), the characteristic bonds at 1100 cm^{-1} (Si–O) indicates silica coating on the surface of the MNPs [39-41].

In the Hercynite@SiO_2-APTS spectrum (Fig. 1c), the appearance of a double band in the region of 3300-3400 cm^{-1} related to NH_2 group indicates the addition of APTS to the Hercynite@SiO_2. The spectrum of proline (Fig. 1d) absorption band in the region of 1700 cm^{-1} corresponds to the carbonyl group and the broad peak in the region of 3000-3500 cm^{-1} corresponds to the carboxylic acid group. Also, the peaks at 1356 and 1464 cm^{-1} are related to the bending vibration of N–H. Comparing Fig. 1e (Hercynite@SiO_2-APTS-Proline) with Fig. 1c and Fig. 1d shows that the double band related to the amino group in Fig 1e disappeared, in comparison with Fig. 1c, and the carbonyl group in Fig.1d is weakened and moves the absorption to a lower frequency show that the acidic group of proline has reacted with the amino group of Hercynite@SiO_2-APTS and nano-catalyst Hercynite@SiO_2-APTS-Proline has been synthesized, successfully.

Fig. 2 shows powder x-ray diffraction (P-XRD) of Hercynite and Hercynite@SiO_2-APTS-Proline. As it can be seen, the successful synthesis of hercynite MNPs was justified by the XRD peak positions at 2θ =30.59, 32.15, 35.99, 43.65, 45.87, 54.11, 57.61, 63.27, 71.81, 74.65 and 75.70, which are related to (2 0 0), (0 3 1), (3 1 1), (4 0 0), (1 1 0), (4 2 2), (1 1 1), (4 4 0), (6 2 0), (5 3 3) and (1 1 1) reflections, respectively [35]. Also, the similarity of the XRD pattern of Hercynite@SiO_2-APTS-Proline with hercynite, shows that it has an octahedral structure. However, the two high order (0 3 1) and (1 1 0) diffraction peaks disappeared, indicating the peak reflections originating from the core magnetite.

Energy dispersive X-ray (EDX) analysis of Hercynite@SiO_2-APTS and Hercynite@SiO_2-APTS-Proline MNPs is shown in Fig 3. Presence of elements of C (33.7 w % O (26.6 w %),), Fe (23.4 w %), Si (7.1 w %), N (6.1 w %) and Al (3.1 w %) in the structure of synthesized Hercynite@SiO_2- APTMS (Fig. 3a) and existence of C (34.2 w %), O (26.6 w %), Fe (22.2w %), Si (6.1 w %), N (7.9 w %) and Al (3.0 w %) elements in the structure of synthesized Hercynite@SiO_2-APTS-Proline MNPs confirms that the mentioned structures have been successfully synthesized. The comparison of Fig. 3a and 3b shows that the decrease in the percentage of Fe, Si, Al elements and an increase percentage of carbon and nitrogen elements in Hercynite@SiO_2-APTS-Proline is due to the binding of proline on the structure of Hercynite@SiO_2-APTS MNPs.

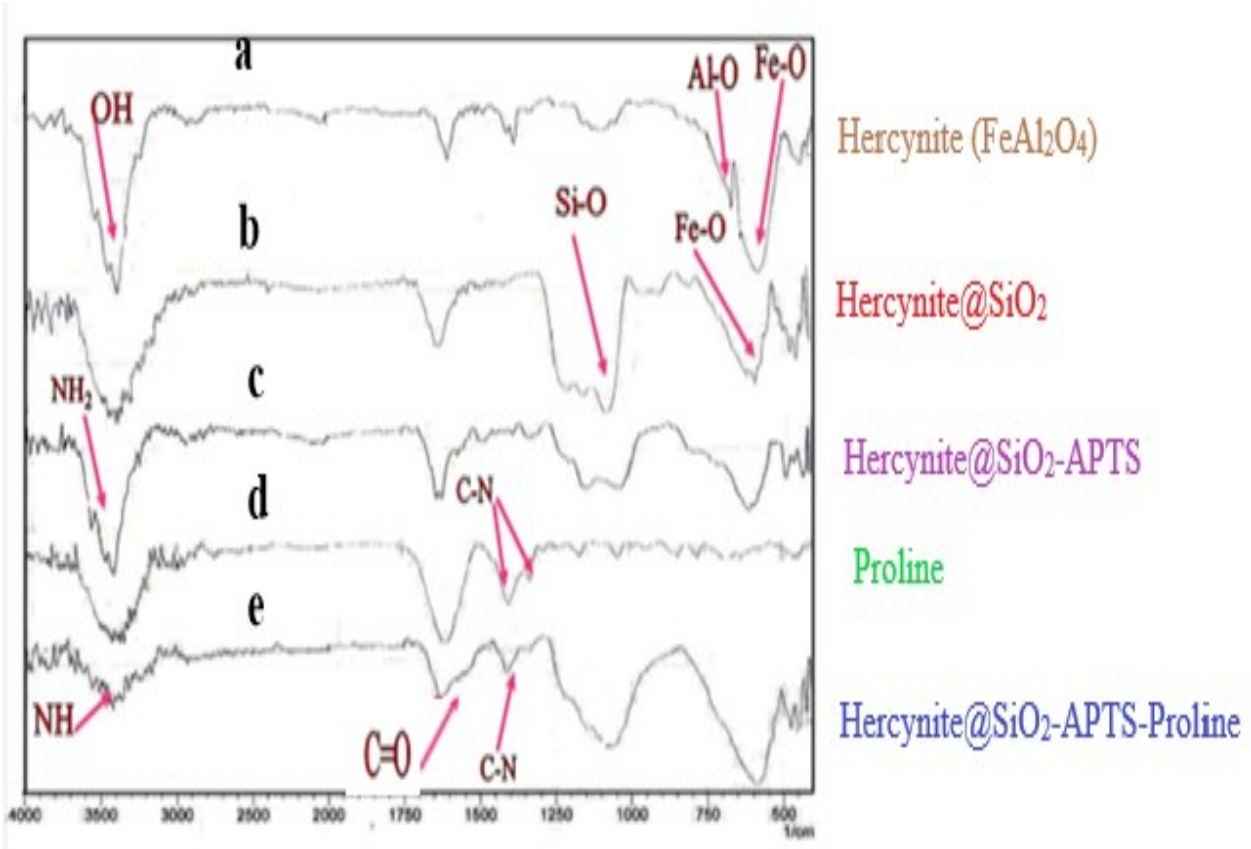

Figure 1. FT-IR spectra of Hercynite (1a), Hercynite@SiO_2 (1b), Hercynite@SiO_2-APTS (1c), Proline (1d) and Hercynite@SiO_2-APTS-Proline MNPs (1e)

10.57647/ijc.2026.1602.18

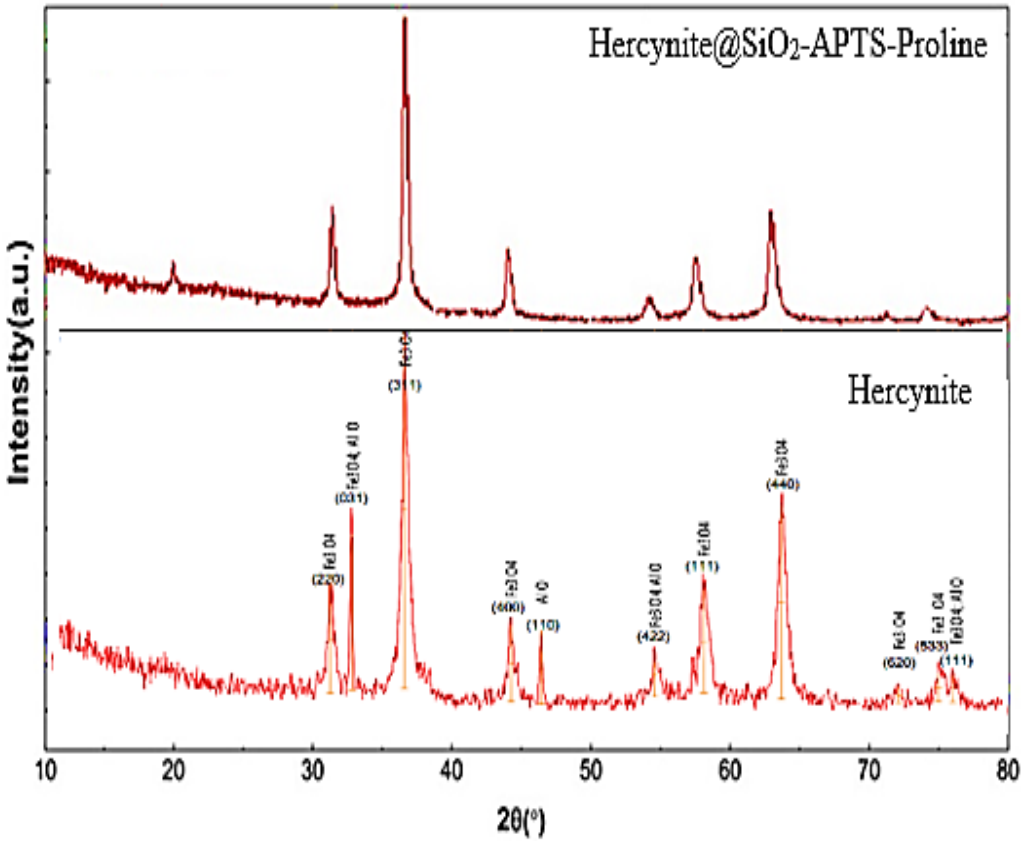

Figure 2. P-XRD patterns of Hercynite and Hercynite@SiO_2-APTS-Proline

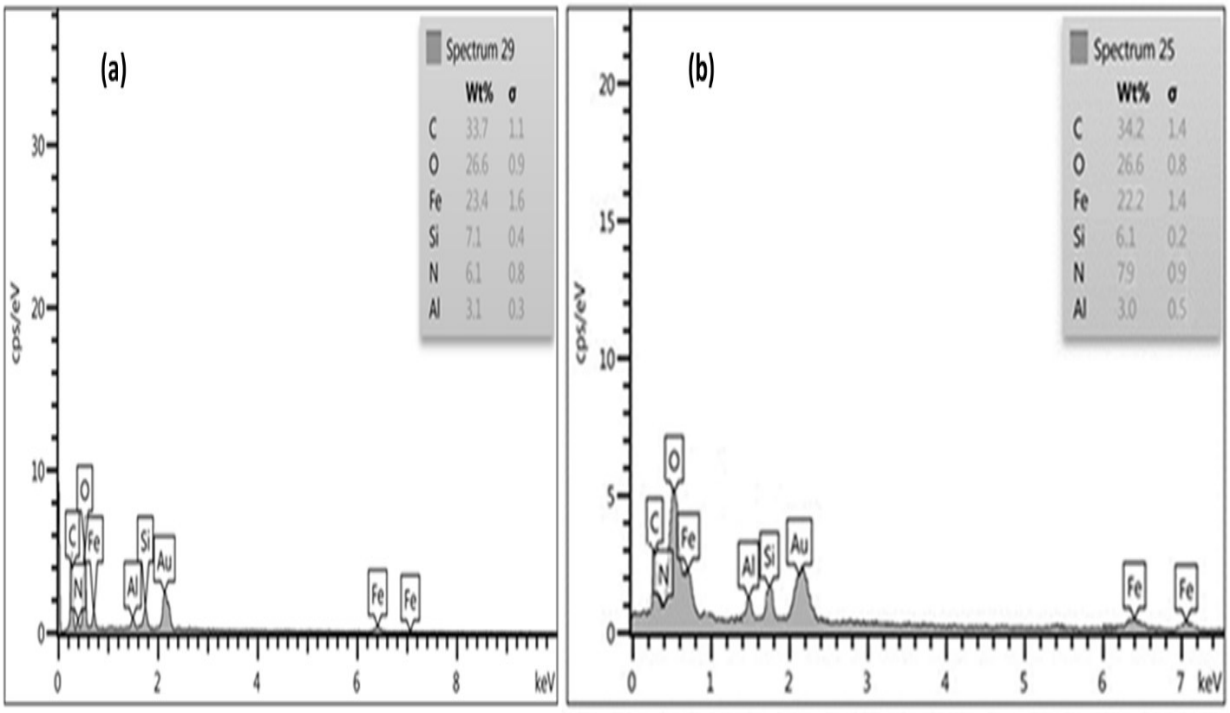

Figure 3. Energy dispersive X-ray (EDX) analysis of Hercynite@SiO_2-APTS (a) and Hercynite@SiO_2-APTS-Proline (b)

Scanning electron microscopy (SEM) techniques (Fig. 4), shows the spherical morphology for the hercynite (Fig. 4a) and Hercynite@SiO_2-APTS (Fig. 4b) which consist of a series of regular particles having a mean diameter of 29–78 nm. The transmission electron microscopy (TEM) images for the hercynite (Fig. 4c) and Hercynite@SiO_2-APTS (Fig. 4d) were studied and the uniform spherical nanoparticles with a dark core surrounded by a light shell in Fig. 4d confirmed the presence of APTS-Proline shell on the core of hercynite.

10.57647/ijc.2026.1602.18

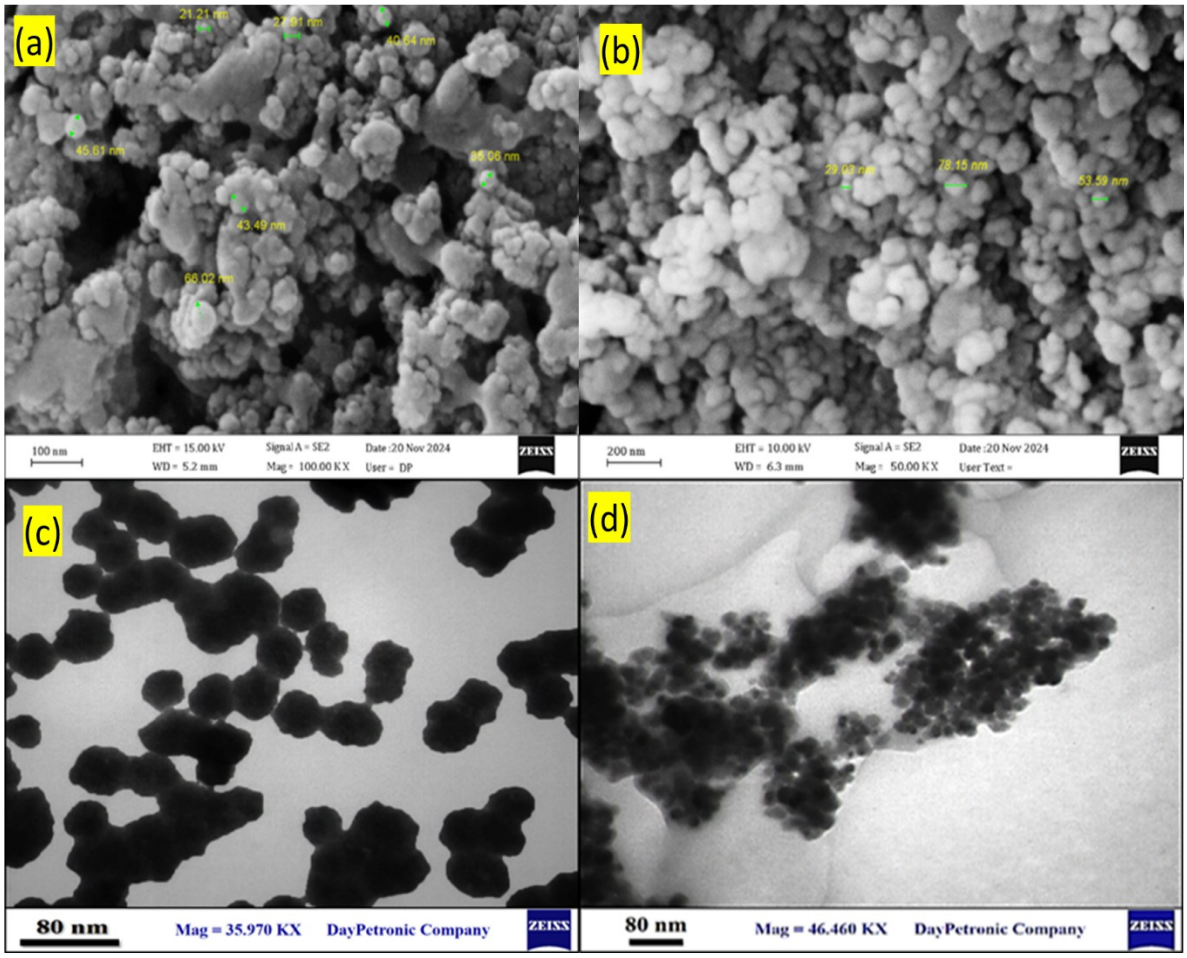

Figure 4. SEM and TEM images for Hercynite (a, c) and Hercynite@SiO_2-APTS MNPs (b,d)

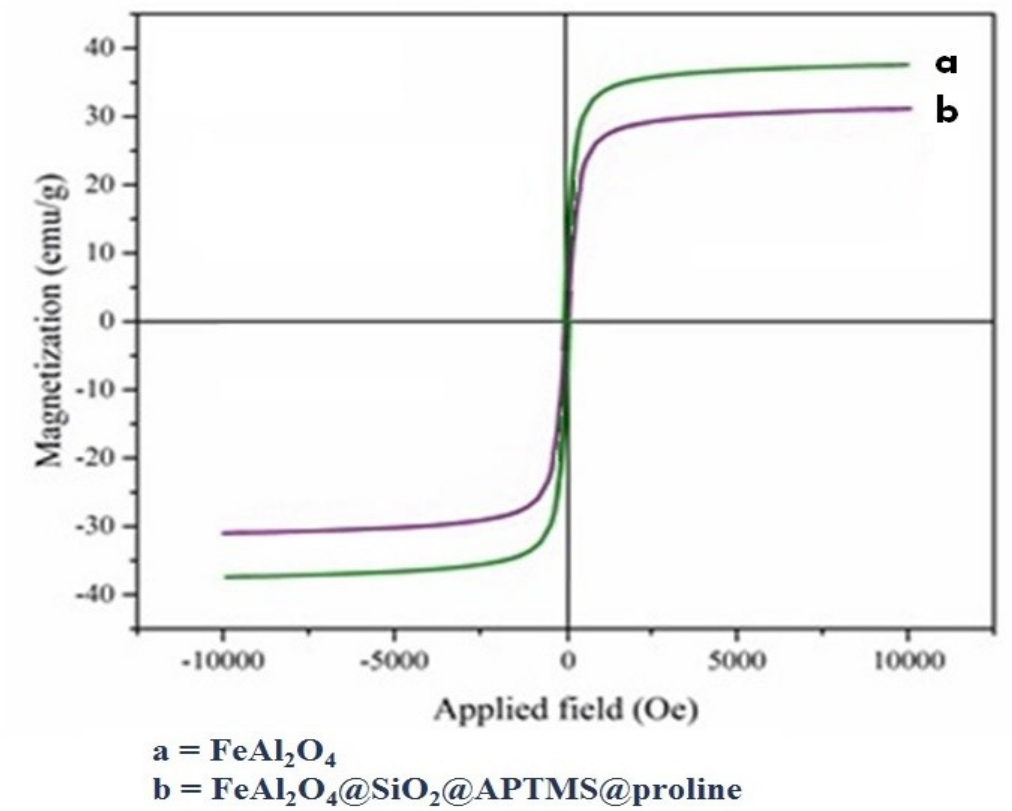

Figure 5. Magnetic hysteresis curves of (a) hercynite and (b) Hercynite@SiO_2-APTS-Proline

10.57647/ijc.2026.1602.18

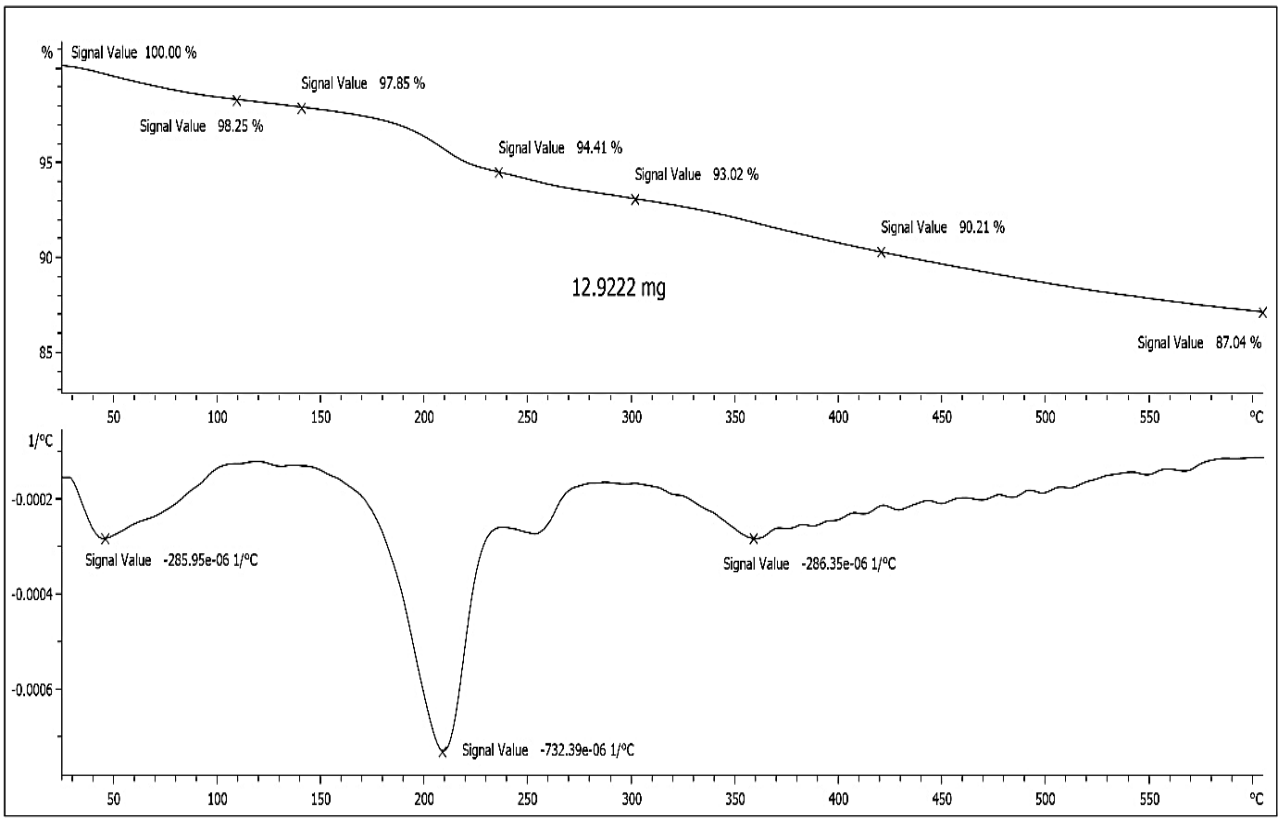

Figure 6. TGA-DSC curve of Hercynite@SiO_2-APTS-Proline

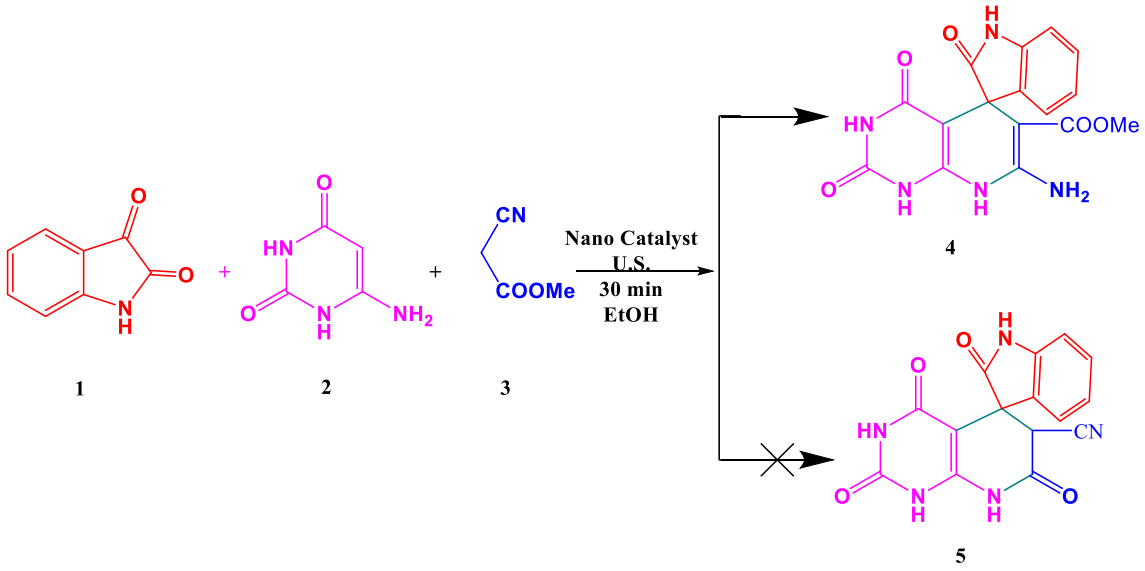

Scheme 2. Synthesis of spiro[indoline-3,5'-pyrido[2,3-*d*] pyrimidine]

The magnetic hysteresis curves of the hercynite and Hercynite@SiO_2-APTS-Proline (Fig. 5) show that both of them are superparamagnetic with distinct magnetic properties at room temperature. The saturation magnetization values for the hercynite and Hercynite@SiO_2-APTS-Proline are about 39 and 35 emu g^{-1}, respectively. The decrease in magnetism in Hercynite@SiO_2-APTS-Proline due to the coating of APTS and proline shell over the magnetic hercynite core.

Fig. 6 shows the TGA-DSC curve of Hercynite@SiO_2-APTS-Proline, with a total weight loss 12.96%. The weight loss at below 150 and endothermic peak near 50 °C is related to the removal of water and other organic solvents. Also, the weight lost in the region of 150-350 endothermic peak near 200 °C is related to the decomposition of APTS-Proline. These results show organic catalytic layer (APTS-Proline) grafted on Hercynite@SiO_2.

3.2. Catalytic studies

After synthesizing and confirming the structure of Hercynite@SiO_2-APTS-Proline, its efficiency as catalyst was investigated for multicomponent reaction of 6-

10.57647/ijc.2026.1602.18

aminouracile, isatin and methylcyanoacetate. The possibility of carrying out the desired reaction under two conditions of reflux and ultrasound irradiation in the presence of different amounts of catalyst was investigated and compared with other catalysts (Table 1). The results showed that in both methods, which are likely to consist of products 4 and 5, compound 4 is the main product and the catalyst causes the reaction to be carried out in a regioselective manner (Scheme 2). Also, catalyst Hercynite@SiO_2-APTS-Proline gives better results than other catalysts in both reflux and ultrasound methods.

3.3. Reusability of catalysts

Also, reusability of Hercynite@SiO_2-APTS-Proline MNPs as catalyst was studied on the model reaction. After the reaction is complete, the catalyst is separated (about 95% of the original amount) and washed several times with ethanol and drying at 100 °C and reused to perform the reaction five times. As shown in Fig. 7, with each reuse of the catalyst, the reaction yield is slightly reduced, but the amount of product obtained is acceptable (run 1, 92%; run 2, 90%; run 3, 87%; run 4, 83%; run 5, 81%) which shows the stability of the catalyst after 5 recycles. Also, comparison of FT-IR and XRD of the Hercynite@SiO_2-APTS-Proline before and after use for the synthesis of 4a confirms that no changes were made to the catalyst structure (Fig. 8, 9). After study of recycling of Hercynite@SiO_2-APTS-Proline MNPs, finally turn over number (TON) and turn over frequency (TOF) of the present catalyst were also calculated for the model reaction based on the synthesis of 4a; they were found to be 625.39 and 327.63 h^{-1}, respectively.

Table 1. Screening of reaction condition for the synthesis of 4a

entry	Catalyst	Amount of catalyst	Reflux		Ultrasound (60 ^{0}C)	
			Time (min)	Yield (%)	Time (min)	Yield (%)
1	Non-Cat	-	480	-	120	-
2	CH_3COOH	0.5 mmol	240	58	140	62
3	Alum	0.5 mmol	200	74	120	64
4	$AlCl_3$	0.5 mmol	220	43	120	43
5	Hercynite	0.5 mmol	180	45	120	56
6	L-Proline	0.5 mmol	180	58	60	70
7	$FeAl_2O_4$@SiO_2-APTMS-proline	0.1 g	120	85	30	93
8	$FeAl_2O_4$@SiO_2-APTMS-proline	0.07 g	120	82	30	92
9	$FeAl_2O_4$@SiO_2-APTMS-proline	0.05 g	150	55	40	78
10	$FeAl_2O_4$@SiO_2-APTMS-proline	0.03 g	170	45	50	55

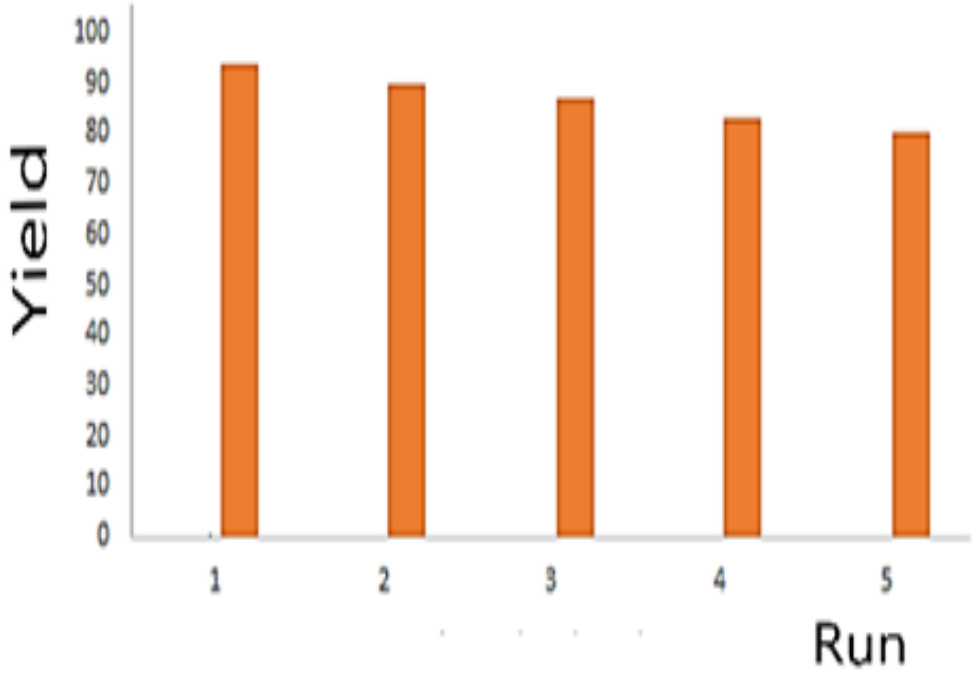

Figure 7. Reusability of catalyst for synthesis of 4a

10.57647/ijc.2026.1602.18

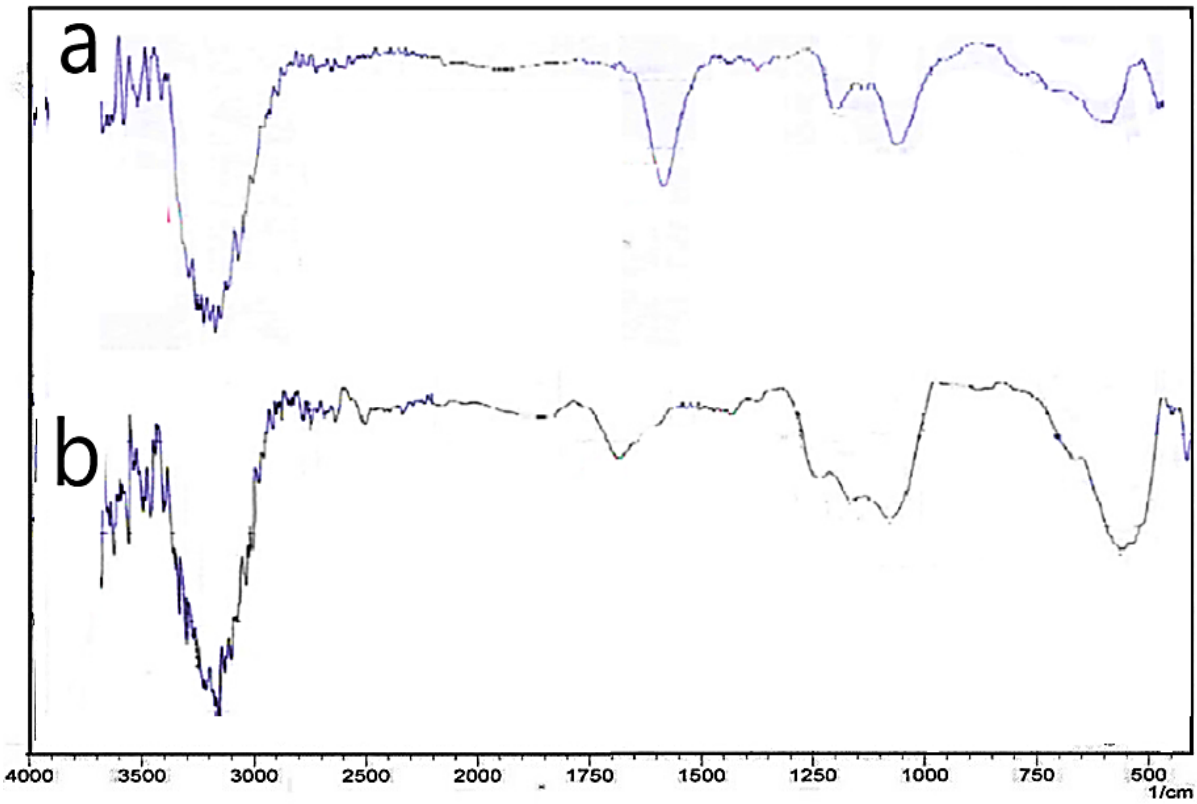

Figure 8. FT-IR of the Hercynite@SiO_2-APTS-Proline before (8a) and after use (8b) for the synthesis

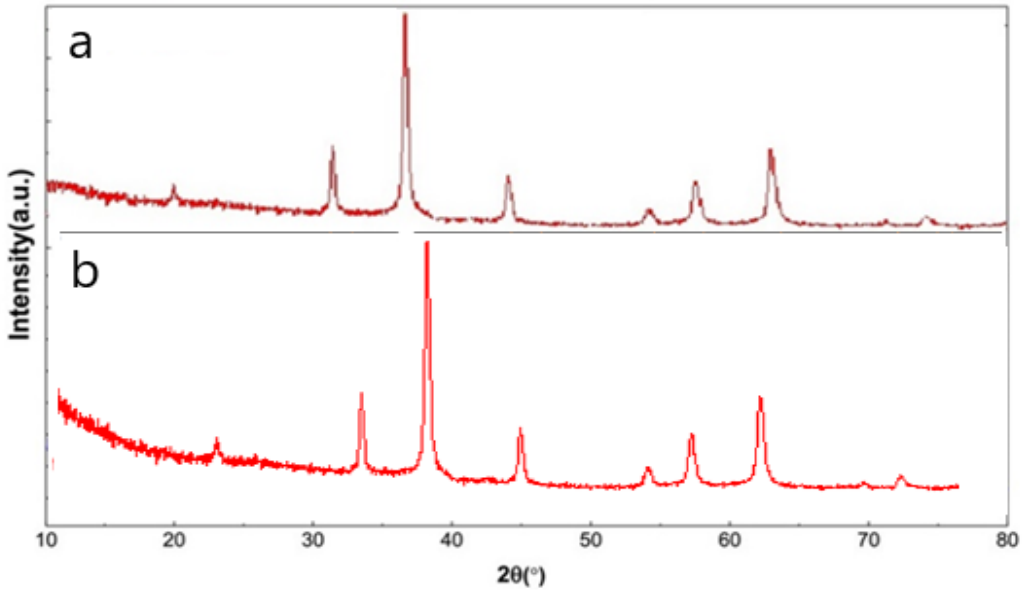

Figure 9. XRD of the Hercynite@SiO_2-APTS-Proline before (8a) and after use (8b) for the synthesis of 4a

3.4. The hot filtration test

The hot filtration test is used for the determination of leaching proline from the catalyst. In the presence of Hercynite@SiO_2-APTS-Proline, synthesis of 4a was done in the optimization condition in halftime of the reaction. The yield of product was 64%. Simultaneously, the synthesis of 4a was done in the same condition, with the difference that the nanocatalyst was removed from the mixture in the halftime of reaction and the reaction was continued. Finally, the yield of reaction was 69%. This result confirmed that the leaching of proline from the heterogeneous catalyst has not been happened.

3.5 A plausible mechanism

According to the proposed mechanism (Scheme 3), the proline part of the catalyst acts as a Schiff base and activates the carbonyl group of isatin to react with uracil and obtain the intermediate 6.

10.57647/ijc.2026.1602.18

Then, methylene group of methyl cyanoacetate reacted with 6 through the Michael addition to afford intermediate 7.

Then, intermediate 7 during the cyclization process and then the tautomerization gives the desired product 4a. After specifying the optimal reaction conditions on the model reaction, the efficiency of catalyst for the synthesis of SIPP (4a-h) and SIPDP (9a-e) derivatives through the reaction of 6-aminouracil with isatin derivatives and ethyl cyanoacetate or barbituric acid under ultrasonic condition was evaluated and the results are shown in Scheme 4 and Table 2.

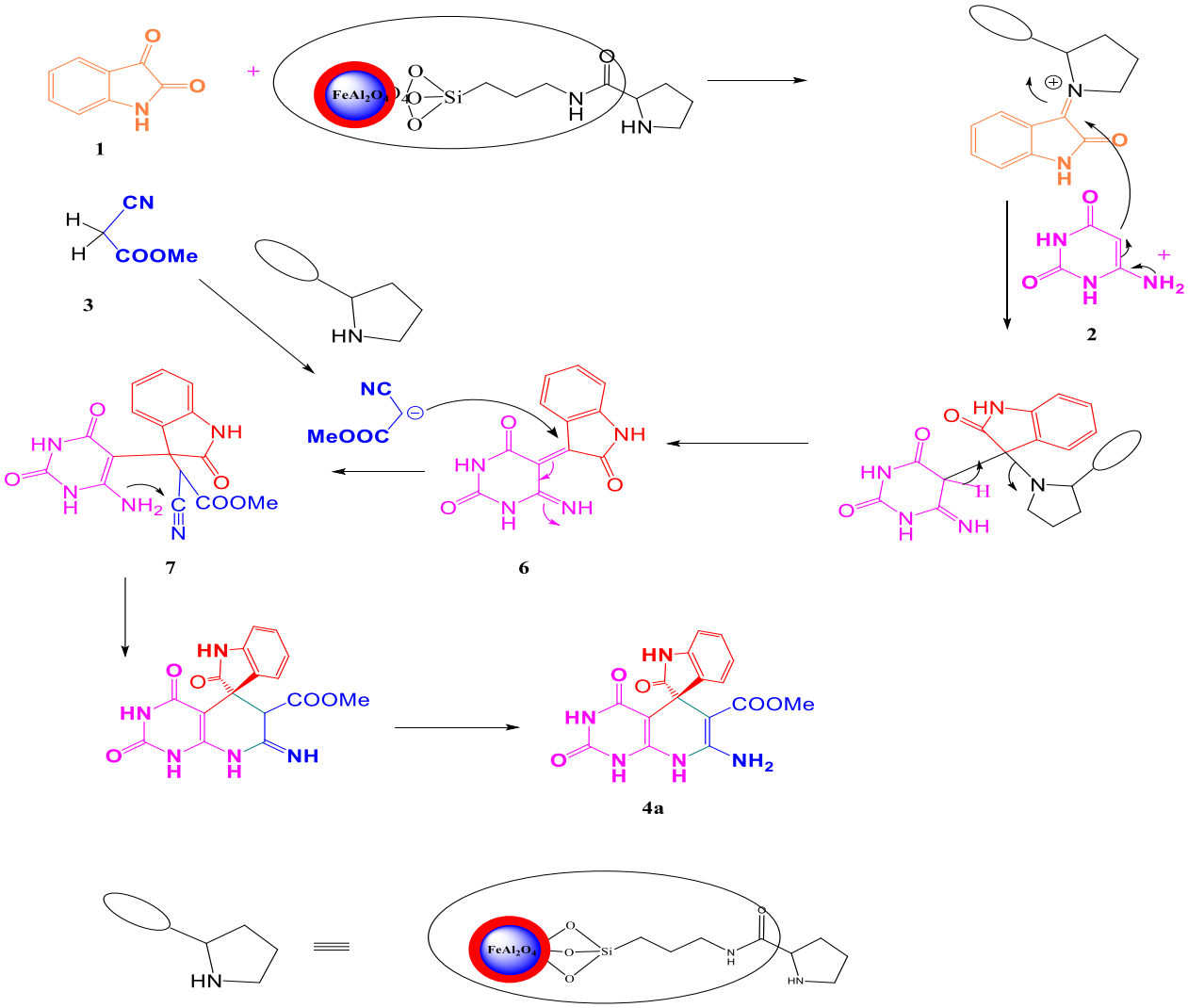

Scheme 3. Proposed mechanism for the synthesis of 4a in the presence of catalyst Hercynite@SiO_2-APTS-Proline

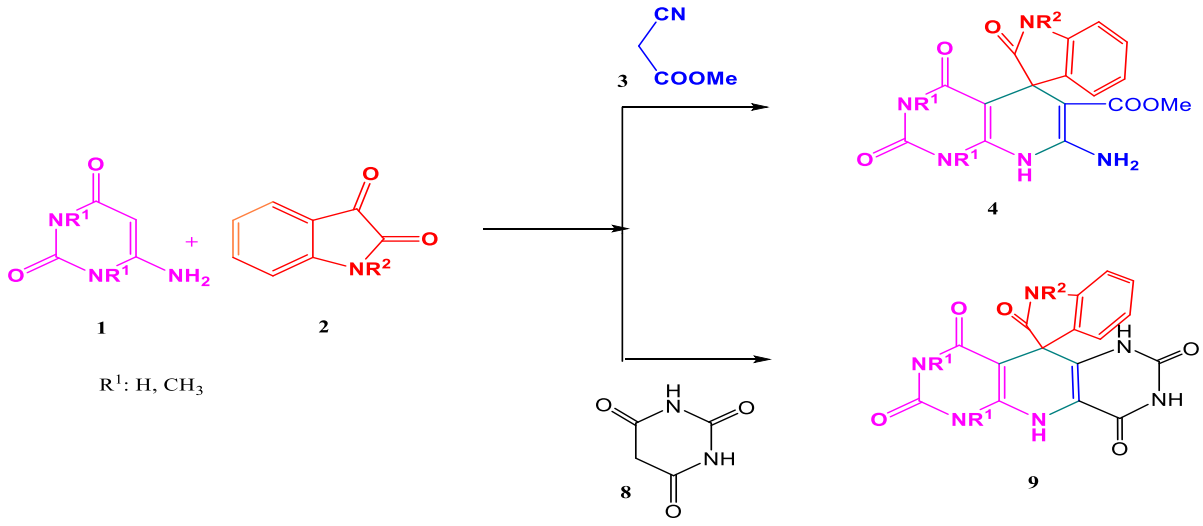

Scheme 4. Synthesis of SIPP (4a-h) and SIPDP (9a-e) derivatives

10.57647/ijc.2026.1602.18

Table 2. Synthesis of SIPP (4a-h) and SIPDP (9a-e) derivatives

Entry	Products	Reflux		Ultrasound		M.P (°C)
		Time (min)	yield (%)	Time (min)	yield (%)	
4a	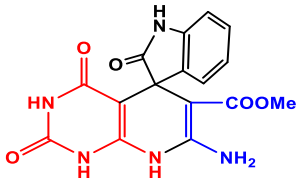	120	82	30	92	300-302
4b	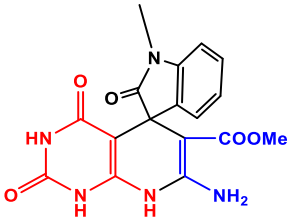	155	80	35	89	340-342
4c	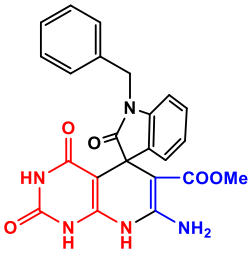	160	78	40	72	305-307
4d	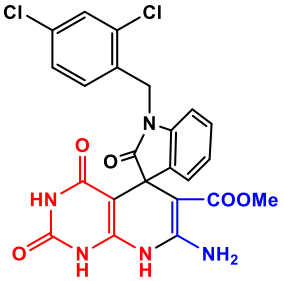	155	85	35	90	342-344
4e	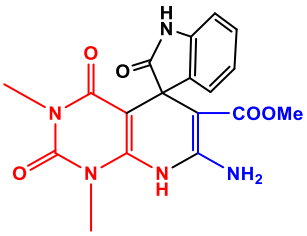	150	80	35	92	301-304
4f	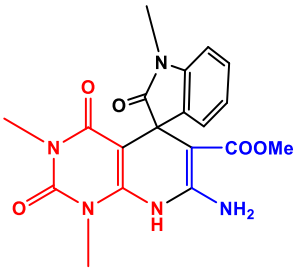	180	72	40	86	342-345
4g	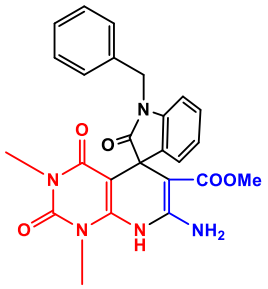	200	60	60	70	307-310

Table 2. Synthesis of SIPP (4a-h) and SIPDP (9a-e) derivatives (continued)

Entry	Products	Reflux		Ultrasound		M.P (°C)
		Time (min)	yield (%)	Time (min)	yield (%)	
4h	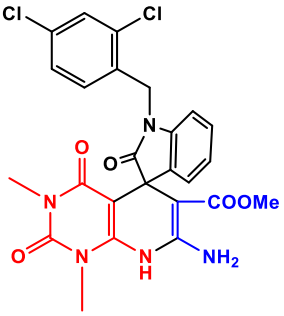	180	85	45	90	344-347
9a	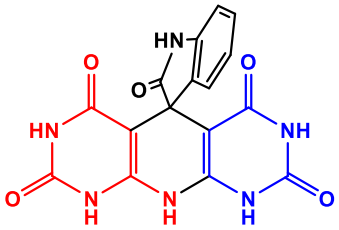	190	70	120	76	324-326
9b	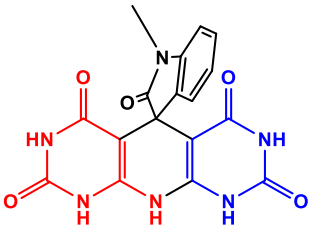	190	65	90	75	372-375
9c	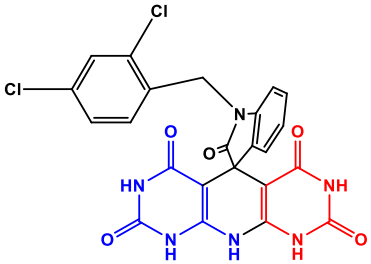	250	70	110	87	366-368
9d	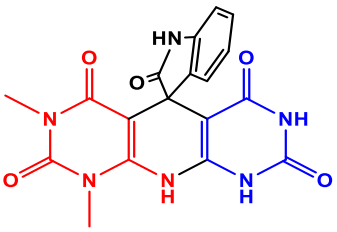	260	65	170	70	327-330
9e	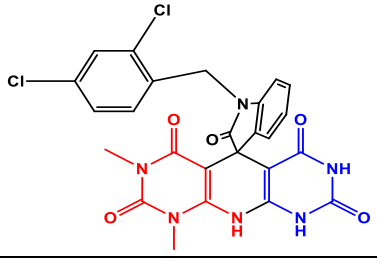	220	70	80	80	368-371

4. Conclusion

In this research, for the first time, a facile method for the synthesis of Hercynite@SiO_2-APTS-Proline as a novel magnetic nano particle was successfully designed. The structure and composition of the prepared magnetic nano particle were completely characterized by FT-IR, XRD, EDX, SEM, TEM, TGA and VSM techniques. Moreover,

10.57647/ijc.2026.1602.18

the catalytic activity of this nanocomposite was investigated for the synthesis of SIPP (4a-h) and SIPDP (9a-e) derivatives. High surface area, convenient recoverability, reusability for several times without any significant loss of catalyst activity, the use of a commercially available materials, operational simplicity, ease of separation by simple filtration, cheap and chemically stabile reagents, good reaction times, simple practical methodology and ease of use make the prepared catalyst a promising candidate for potential applications in some organic reactions. The possibility of forming a complex with metals and organic pigments and removing them is one of the other features of this synthesized nanoparticle.

Funding Declaration
No funding was received from any governmental or non-governmental organization to conduct this research.

Data availability
All the data generated or obtained from analyses of this study are included in the article and its supplementary information file.

Supplementary information
FT-IR, ^{1}H- and ^{13}C-NMR all of the compounds are available in the supplementary.

References

[1] P. Jahanshahi, M. Mamaghani, F. Haghbin, R. Hossein Nia, M. Rassa, *J. Mol. Struct.,* **1155**(2018): 520-529, https://doi.org/10.1016/j.molstruc.2017.11.034

[2] R. Naresh Kumar, G. Jitender Dev, N. Ravikumar, D. Krishna Swaroop, B. Debanjan, G. Bharath, B. Narsaiah, S. Nishant Jain, A. Gangagni, *Bioorg. Med. Chem. Lett.,* **26**(2016): 2927-2930, https://doi.org/10.1016/j.bmcl.2016.04.038

[3] B. Hurlbert, B. Valenti, *J. Med. Chem.,* **11**(1968):708-710, https://doi.org/10.1021/jm00310a016

[4] J. Quiroga, C. Cisneros, B. Insuasty, R. Abonia, S. Cruz, M. Nogueras, J. M. Torre, M. Sortino, S. Zacchino, *J. Het. Chem.,* **43**(2006):299-306, https://doi.org/10.1002/jhet.5570430208

[5] M. Ghorab, A. Hassan, *Phosph. Sulf. Silic. Relat. Elem.,* **141**(1998):251-261, https://doi.org/10.1080/10426509808033737

[6] X. Gao, L. Cen, F. Li, R. Wen, H. Yan, H. Yao and S. Zhu, *Biochem. Biophys. Res. Commun.,* **505**(2018):1-7, https://doi.org/10.1016/j.bbrc.2018.09.120

[7] A. Rosowsky, C. E. Mota, S. F. Queener, *J. Het. Chem.,* **32** (1995) 335-340, https://doi.org/10.1002/jhet.5570320155

[8] A. A. Eissa, K. F. Aljamal, H. S. Ibrahim, H. A. Allam, *Bioorg. Chem.,* **116**(2021):105318-105328, https://doi.org/10.1016/j.bioorg.2021.105318

[9] M. Kidwai, S. Saxena, S. Rastogi, *Curr. Med. Chem.*, **2**(2003):269-286. https://doi.org/10.2174/1568012033483015

[10] A. Gangjee, H. D. Jain, J. Phan, X. Lin, *Med. Chem.*, **49**(2006):1055-1065. https://doi.org/10.1021/jm058276a

[11] E. M. Grivsky, S. Lee, C. W. Sigel, D. S. Duch, *J. Med. Chem.*, **23**(1980):327-329. https://doi.org/10.1021/jm00177a025

[12] V. J. Ram, A. Goel, S. Sarkhel, P. R. Maulik, *Bioorg. Med. Chem.,* **10**(2002):1275-1280. https://doi.org/10.1016/S0968-0896(01)00423-0

[13] Y. S. Sanghvi, S. B. Larson, S. S. Matsumoto, L. D. Nord, D. F. Smex, R. C. Willis, T. H. Avery, R. K. Robins, G. R Revankar, *J. Med. Chem.*, **32**(1989):3629.

[14] F. Himo, T. Lovell, R. Hilgraf, V. V. Rostovtsev, L. Noodleman, K. B. V. V. Sharples, *J. Am. Chem*. Soc., **127**(2005):210-216. https://doi.org/10.1021/ja0471525

[15] C. W. Tornoe, C. Christensen, M. Melda, *J. Org. Chem.*, **67**(2002):3057-3064. https://doi.org/10.1021/jo011148j

[16] R. Baharfar, R. A Azimi, *Chin. Chem. Lett*., **22**(2011):1183-1186. https://doi.org/10.1016/j.cclet.2011.04.020

[17] S. Samai, G. C. Nandi, S. Chowdhury, M. S. Singh, *Tetrahedron*, **67**(2011):5935-5941. https://doi.org/10.1016/j.tet.2011.06.051

[18] M. Y. Jang, S. D. Jonghe, L. G. Gaob, P. Herdewijn, *Tetrahedron Lett*. **47**(2006): 891-8920. https://doi.org/10.1016/j.tetlet.2006.10.056

[19] B. R. Thorat, S. N. Mali, S. S. Wavhal, D. S. Bhagat, R. M. Borade, A. Chapolikar, A. Gandhi, P. Shinde, *Comb. Chem. & High Through. Screen.,* **26**(2023):1108-1140. https://doi.org/10.2174/1386207325666220720105845

[20] M. S. Shafik, H. J. Elaibi, *Nanomater Chem.,* **2**(2024):51-65. https://doi.org/10.22034/nc.2024.460096.1033

[21] A. S. M. Ivana Lago, *J. Synth. Chem.*, **3**(2024):24-35. https://doi.org/10.22034/jsc.2024.456522.1072

[22] M. Jalili, M. Salehpour *Biol. Mol. Chem.*, 2(2024):108-122. https://doi.org/10.22034/bmc.2024.491601.1043

[23] F. Montazery, R. Baharfar, B. Maleki, *J. Sci.: Adv. Mat. Devic.,* 10(2025):100958. https://doi.org/10.1016/j.jsamd.2025.100958

[24] Z. Valipour, R. Hosseinzadeh, Y. Sarrafi, B. Maleki, *Scientific Rep.,* 15(1) (2025):40184-40200. https://doi.org/10.1038/s41598-025-23849-4

[25] S. Peiman, B. Maleki, *Scientific Rep.*, 14(1) (2024):17401-17420. https://doi.org/10.1038/s41598-024-68316-8

[26] H. Kefayati, K. Rad-Moghadam, M. Zamani, S. Hosseyni, *Let. Org. Chem.,* **7**(2010): 277-282. https://doi.org/10.2174/157017810791130577

[27] H. Kefayati, S. Khandan, S. Tavancheh, *Russ. J. Gen. Chem.* **85**(2015):1757-1762. https://doi.org/10.1134/S1070363215070300

[28] S. Nikzad Shalkouhi, H. Kefayati, Sh Shariati, *J. Iran. Chem. Soc.*, **16**(2019):263–2677. https://doi.org/10.1007/s13738-018-1506-9

[29] R. R. Kazemi-Rad, J. Azizan, H. Kefayati *J. Serb. Chem. Soc*., **81**(2016):29–34. https://doi.org/10.2298/JSC150210048K

[30] H. Kefayati, S. Jirsaray Bazargard, P. Vejdansefat, Sh. Shariati, A. Mehtar Kohankar. *Dyes and Pig.,* **125**(2016):309-315. https://doi.org/10.1016/j.dyepig.2015.10.034

[31] F. Tajali Rad, H. Kefayati, Sh Shariati, *App. Organometal. Chem.,* **33**(2019):2 e 4732-4743. https://doi.org/10.1002/aoc.4732

[32] S. Mousavifar, H. Kefayati, and Sh Shariati, *App. Organometal. Chem.,* **32**(2018):4 e 4242-4253. https://doi.org/10.1002/aoc.4242

[33] S. Nikzad Shalkouhi, H. Kefayati, Sh Shariati, *Iran. J. Cat*., **8**(2018):213-20. https://oiccpress.com/ijc/article/view/4005

[34] S. C. Azimi, H. Kefayati, *Iran. J. Cat.,* 3(2013):123-128. https://oiccpress.com/ijc/article/view/3763

[35] A. Ghorbani-Choghamarani, M. Mohammadi, L. Shiri, Z. Taherinia, Res. Chem. Intermed., **45**(2019):5705-5723. https://doi.org/10.1007/s11164-019-03930-0

[36] S. Rezayati, A. Ramazani, S. Sajjadifar, H. Aghahosseini, A. Rezaei, *ACS Omega,* **6**(2021):25608-25622. https://doi.org/10.1021/acsomega.1c03672

[37] P. M. Botta, R. C. Mercader. *Scripta Materialia*, **48**(2003):1093-1098. https://doi.org/10.1016/S1359-6462(02)00630-9

[38] M. Mohammadi, A. Ghorbani-Choghamarani, *RSC Adv*., **12**(2022):2770-2787. https://doi.org/10.1039.D1RA07381H

[39] V. Umamaheswari, *J. Catal*., **210**(2002):367-374. https://doi.org/10.1006/jcat.2002.3709

[40] F. Hajizadeh, A. B. Amiri, F. Maleki, Z. Mohammadi. *Microchem. J*., **175**(2022):107176. https://doi.org/10.1016/j.microc.2022.107176

[41] A. Ghorbani-Choghamarani, H. Aghavandi, M. Mohammadi *Appl. Organomet. Chem.,* **34**(2020):5804-5815. https://doi.org/10.1002/aoc.5804